Cardiac myosin activation with 2-deoxy-ATP via increased electrostatic interactions with actin

Joseph D. Powers[a,b,1,2], Chen-Ching Yuan[a,1], Kimberly J. McCabe[b], Jason D. Murray[a,c], Matthew Carter Childers[a], Galina V. Flint[a], Farid Moussavi-Harami[d], Saffie Mohran[a], Romi Castillo[a], Carla Zuzek[a], Weikang Ma[e], Valerie Daggett[a], Andrew D. McCulloch[b], Thomas C. Irving[e], and Michael Regnier[a,c,2]

[a]Department of Bioengineering, University of Washington, Seattle, WA 98109; [b]Department of Bioengineering, University of California, San Diego, La Jolla, CA 92093; [c]Department of Physiology and Biophysics, University of Washington, Seattle, WA 98109; [d]Division of Cardiology, Department of Medicine, University of Washington, Seattle, WA 98109; and [e]Department of Biological Sciences, Illinois Institute of Technology, Chicago, IL 60616

Edited by Yale E. Goldman, University of Pennsylvania, Philadelphia, PA, and approved April 29, 2019 (received for review March 25, 2019)

The naturally occurring nucleotide 2-deoxy-adenosine 5′-triphosphate (dATP) can be used by cardiac muscle as an alternative energy substrate for myosin chemomechanical activity. We and others have previously shown that dATP increases contractile force in normal hearts and models of depressed systolic function, but the structural basis of these effects has remained unresolved. In this work, we combine multiple techniques to provide structural and functional information at the angstrom-nanometer and millisecond time scales, demonstrating the ability to make both structural measurements and quantitative kinetic estimates of weak actin–myosin interactions that underpin sarcomere dynamics. Exploiting dATP as a molecular probe, we assess how small changes in myosin structure translate to electrostatic-based changes in sarcomere function to augment contractility in cardiac muscle. Through Brownian dynamics simulation and computational structural analysis, we found that deoxy-hydrolysis products [2-deoxy-adenosine 5′-diphosphate (dADP) and inorganic phosphate (Pi)] bound to prepowerstroke myosin induce an allosteric restructuring of the actin-binding surface on myosin to increase the rate of cross-bridge formation. We then show experimentally that this predicted effect translates into increased electrostatic interactions between actin and cardiac myosin in vitro. Finally, using small-angle X-ray diffraction analysis of sarcomere structure, we demonstrate that the proposed increased electrostatic affinity of myosin for actin causes a disruption of the resting conformation of myosin motors, resulting in their repositioning toward the thin filament before activation. The dATP-mediated structural alterations in myosin reported here may provide insight into an improved criterion for the design or selection of small molecules to be developed as therapeutic agents to treat systolic dysfunction.

myosin structure | dATP | X-ray diffraction | sarcomere structure | electrostatics

Heart failure (HF) is a chronic progressive condition in which the heart is unable to pump blood throughout the body at normal filling pressures, and it is a significant and growing medical challenge. Current treatments only slow progression of HF and do not rescue cardiac muscle function. Consequently, there is a pressing need for novel therapeutic interventions that enhance cardiac contractility in failing hearts.

Cardiac muscle contraction is generated at the molecular level by cyclical, adenosine 5′-triphosphate (ATP)–driven actin–myosin interactions, making myosin an appealing therapeutic target for treating ventricular systolic dysfunction. Accordingly, there are several myosin-specific small-molecule compounds currently being developed and tested to treat HF. One is the naturally occurring ATP analog 2-deoxy-ATP (denoted dATP). We have previously demonstrated that dATP can be used by cardiac myosin in place of ATP as the substrate that fuels actin–myosin cross-bridge cycling (1). Moreover, we have shown that dATP increases contractility in rat myocardium (1), improves left ventricular function in a porcine model of myocardial infarction (2), and increases contractility of ventricular muscle from patients in human end-stage HF (3). Chemomechanical studies suggest that the dATP-mediated force augmentation occurs by increasing cross-bridge binding and cycling rates (4–7), but a precise structural explanation for this is lacking. A recent computational study using molecular dynamics simulations suggests that dATP behaves as an allosteric effector of prepowerstroke myosin, such that when 2-deoxy-adenosine 5′-diphosphate and inorganic phosphate (dADP.Pi) are in the nucleotide binding pocket, local structural changes lead to exposure of more positively charged residues on the actin-binding surface of myosin compared withADP.Pi (8). This led us to hypothesize that dATP increases the electrostatic

Significance

The development of several small-molecule myosin activators to rescue cardiac contractility of failing hearts is underway, but understanding the multiscale structure-function consequences of these inotropes remains a major challenge. Using 2′-deoxy-adenosine 5′-triphosphate (dATP; a myosin-binding nucleotide) as a molecular probe, we show that a restructuring of prepowerstroke myosin in the presence of 2-deoxy-adenosine 5′-diphosphate and inorganic phosphate (dADP.Pi) (versus ADP.Pi) increases actin–myosin electrostatic interactions and binding kinetics. X-ray diffraction revealed myosin structure with dATP in relaxed myofilament is similar to the activated state with ATP, with S1 head movement toward actin and stabilization, resulting in an improved probability of strong cross-bridge formation upon activation. Thus, the alterations induced by dATP may provide clues to a more optimal structure of cardiac myosin to be attained by myosin-targeted therapies for heart failure.

Author contributions: J.D.P., C.-C.Y., K.J.M., J.D.M., M.C.C., W.M., V.D., A.D.M., T.C.I., and M.R. designed research; J.D.P., C.-C.Y., K.J.M., J.D.M., M.C.C., G.V.F., S.M., R.C., C.Z., W.M., T.C.I., and M.R. performed research; F.M.-H. contributed new reagents/analytic tools; J.D.P., C.-C.Y., K.J.M., J.D.M., M.C.C., G.V.F., S.M., R.C., C.Z., and W.M. analyzed data; and J.D.P. and M.R. wrote the paper.

Conflict of interest statement: M.R. holds an international patent (US Patent 9,868,937 B2) on cell and gene-based methods to improve cardiac function by elevating 2′-deoxy-adenosine 5′-triphosphate. A.D.M. is a cofounder of and has an equity interest in Insilicomed, Inc. and Vektor Medical, Inc., and he serves on the scientific advisory boards. Some of his research grants acknowledged here have been identified for conflict of interest management based on the overall scope of the project and its potential benefit to these entities. The author is required by his institution to disclose this relationship in publications acknowledging the grant support. However, the research subject and findings reported here did not involve the companies in any way and have no relationship whatsoever to the business activities or scientific interests of the companies. The terms of this arrangement have been reviewed and approved by the University of California, San Diego in accordance with its conflict of interest policies. The other authors have no competing interests to declare.

This article is a PNAS Direct Submission.

[1]J.D.P. and C.-C.Y. contributed equally to this work.

[2]To whom correspondence may be addressed. Email: j2powers@ucsd.edu or mregnier@uw.edu.

This article contains supporting information online at www.pnas.org/lookup/suppl/doi:10.1073/pnas.1905028116/-/DCSupplemental.

Published online May 20, 2019.

interactions between cardiac myosin and actin, which may alter the conformation of myosin in the sarcomere to prime myosin for binding to actin and increase cross-bridge formation during activation.

However, assessing how small changes in myosin structure translate to large changes in sarcomere dynamics and contractility is a challenge that requires a combination of multiple techniques that span multiple spatiotemporal scales. As such, we developed an approach to investigate the mechanisms of action of a specific inotropic agent (dATP) with potential therapeutic applications in cardiac muscle that incorporate atomically detailed analysis of molecular structure, Brownian dynamics (BD) simulations of actin–myosin-binding kinetics, and small-angle X-ray diffraction analysis of sarcomere structure. Specifically, atomistic structural models of prepowerstroke myosin-ADP, myosin-dADP, and actin were used to investigate how each nucleotide affects the steric orientation of the actin–myosin-binding surface and the energetics associated with the actin–myosin complex. BD simulations [using Browndye software (9)] of prepowerstroke myosin binding to an actin dimer with either ADP or dADP suggest that dADP-myosin has an increased number of polar residue interactions at the actin–myosin interface compared with ADP-myosin, which is predicted to increase the association kinetics. Next, F-actin filament binding on cardiac myosin-coated surfaces in solutions of varying ionic strength was used to confirm the role of surface charge on actin–myosin binding with ATP vs. dATP experimentally. Finally, the results of the X-ray diffraction studies suggest that dATP alters the resting conformation of myosin in the sarcomere, facilitating the movement of the S1 head away from the thick filament backbone and toward actin. Lowering ionic strength (where the surface charge of proteins is increased) reduced the advantage of dATP in facilitating myosin movement, supporting the hypothesis that dATP-induced structural changes in myosin promote myosin–actin interaction via increased electrostatic contacts. Moreover, meridional X-ray diffraction patterns indicated that the resting myofilament structure (i.e., at low calcium) with dATP closely resembles a submaximal active state with ATP. Thus, our multiscale structural and biochemical analysis that couples computational and experimental methods provides a holistic picture of the mechanisms behind augmented cardiac contractility by dATP and represents a framework for characterizing small molecules with potential therapeutic application in ventricular systolic dysfunction.

Results

Electrostatic Restructuring of the Actin–Myosin Interface via dADP.Pi Leads to Increased Binding Kinetics. In prepowerstroke myosin, dADP.Pi allosterically affects myosin, resulting in a structural rearrangement of the nucleotide binding pocket that translates to an altered actin-binding region of myosin (8). However, the effects of the altered actin-binding region of myosin by dADP.Pi on the actin–myosin association kinetics and energetics remained unknown. Here, we used atomically detailed structural representations of actin and myosin to investigate how either dADP.Pi or ADP.Pi (represented as dADP or ADP hereafter) bound to prepowerstroke myosin affects (*i*) the steric orientation and alignment of the actin–myosin interface, (*ii*) the electrostatic potential of the actin–myosin complex, and (*iii*) the actin–myosin-binding kinetics. Fig. 1*A* shows the bound conformation of the actin–myosin complex, with myosin-ADP in red, myosin-dADP in blue, and an actin monomer in green. With dADP bound to myosin, there is a significant increase in the number of residue "contact pairs" (defined as being <3.5 Å apart; *SI Appendix*) compared with myosin-ADP (66 pairs for dADP compared with 49 pairs for the ADP case). Fig. 1*B* depicts the various residue interactions for actin and the actin-binding surface of myosin-ADP (black lines) or myosin-dADP (blue lines), where the thickness of the lines corresponds to the number of atoms in "contact" between the two residues. The diagram highlights the increased actin–myosin interactions in the dADP case via the myosin polar residues ASN 541, LYS 546, HIS 548 and 550, and SER 549 and 552. Moreover, for myosin-dADP, more atomic contact pairs are associated with serine, lysine, and histidine (Fig. 1*C*).

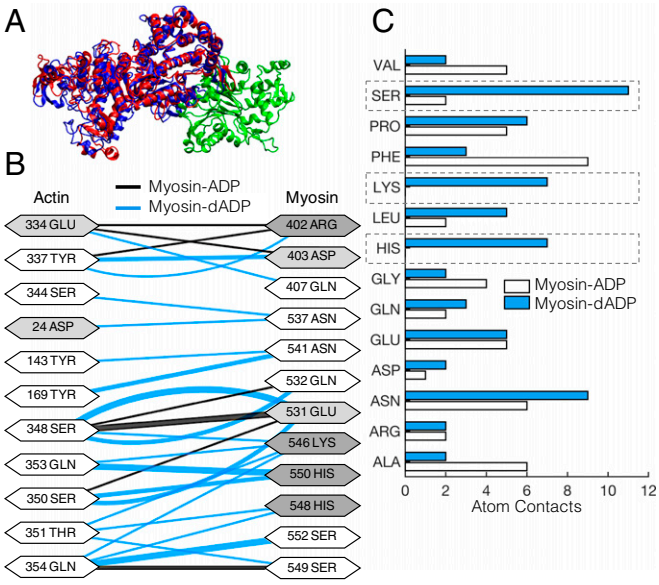

Fig. 1. dADP acts as an allosteric myosin effector to promote polar interactions between actin and prepowerstroke myosin. (*A*) Actin monomer (green) and either ADP-bound (red) or dADP-bound (blue) myosin S1 segments. (*B*) Contact pairs of residues between actin and ADP-bound myosin (black lines) and dADP-bound myosin (blue lines) for an actin–myosin complex. The thickness of the line connecting the interacting residues corresponds to the number of atoms in contact between the residues, and the shading of the residue indicates whether it is polar (white), acidic (light gray), or basic (dark gray). (*C*) Number of atoms in "contact" (discussed in the text) between actin and myosin-ADP (white bars) and myosin-dADP (blue bars) in a prepowerstroke actin–myosin protein complex. There are significant increases in atom contacts that consist of polar residues (SER, LYS, and HIS; highlighted by dashed boxes) between actin and myosin-dADP compared with actin and myosin-ADP.

Bringing more polar residues on myosin into the actin–myosin interaction likely increases the number of hydrogen bonds between myosin and actin, leading to a more stable complex formation. Consistent with this, upon calculating the electrostatic potential (free energy) of the actin–myosin complex for each nucleotide case (*SI Appendix*), we found that the electrostatic potential associated with the actin–myosin protein complex is ~8% lower with dADP bound to myosin compared with ADP (-3.21×10^4 kcal·mol^{-1} versus -2.96×10^4 kcal·mol^{-1}, respectively). Thus, our computational structural analysis [combined with our previous study (8)] predicts that dADP acts as an allosteric myosin effector to directly increase the number of polar interactions between actin and myosin, thereby increasing the electrostatic affinity of myosin for actin. Specifically, we propose that interactions formed by ADP and dADP within the nucleotide binding pocket allosterically result in distinct actin-binding site conformations by altering the dynamics of the switch 1 loop (*SI Appendix*, Figs. S1 and S2).

Based on these results, we hypothesized that increased electrostatic interactions between actin and myosin-dADP will increase the actin–myosin association kinetics. However, given the extremely rapid kinetics of weak cross-bridge binding, it is very difficult to measure the association rates experimentally. Thus, we employed a robust set of BD simulations to estimate second-order bimolecular association rates for the actin–myosin complex with either dADP or ADP bound in the nucleotide binding pocket of myosin (*SI Appendix*). Association rates between actin and ADP-bound or dADP-bound myosin were determined for a wide range of "reaction distance" criteria, defined as the minimum

separation distance between specified atomic contact pairs (as defined above) in the actin–myosin complex required to reach before a reaction was considered to have occurred. We simulated binding of myosin to an actin dimer (500,000 independent trajectories) rather than an actin monomer (as shown in Fig. 1*A*) to provide a more realistic landscape of myosin binding with F-actin while maintaining computational efficiency. Intuitively, association rates are predicted to increase with increased "reaction distance" criteria for either nucleotide (Table 1). Furthermore, as we hypothesized, myosin-dADP is predicted to have a higher association rate with actin compared with myosin-ADP, with the greatest fold change occurring in the range of reaction distance criteria of 1.2–2.5 nm (Table 1). This is likely due to the allosteric response of prepowerstroke myosin to dADP (8) (*SI Appendix*, Figs. S1 and S2) that leads to a more positively charged binding surface of myosin-dADP in the loop 2 region (8) and increased polar hydrogen bonding interactions (Fig. 1), which, together, contribute to a greater electrostatic affinity between actin and myosin and faster association kinetics.

dATP Promotes Electrostatic Interaction of Unregulated Actin Filaments and Cardiac Myosin in Vitro. Next, to experimentally test the hypothesis that dATP promotes electrostatic actin–myosin association (based on the predictions of our BD simulations), we used the in vitro motility (IVM) assay. This assay allows the assessment of actin–myosin interactions and how they are affected by changing conditions (e.g., ionic strength, temperature, pH). In many studies, the ionic strength of motility solutions is maintained between 40 and 100 mM because ionic strength conditions near physiological conditions (~170 mM) tend to disrupt electrostatic interactions, resulting in dissociation of actin from myosin-coated surfaces and floating away in solution (10, 11). However, previous work using IVM assays with heavy meromyosin (HMM) from skeletal muscle demonstrated that as ionic strength was increased (>~100 mM), the fraction of motile actin filaments indeed decreased due to weakened electrostatic interactions with myosin, but the reduction was less with dATP (versus ATP) (8). Because the polar and charge-based surface map differs somewhat between cardiac myosin and fast skeletal muscle myosin, however, it was important to establish whether dATP has similar or different effects with cardiac myosin in the current work. We hypothesized that cardiac HMM would also maintain a higher degree of actin filament interaction with dATP as ionic strength increases. Fig. 2*A* demonstrates this, showing a greater fraction of F-actin interaction (sliding) as ionic strength is increased up to 130 mM. Greater consistency of electrostatic interactions resulted in significantly increased F-actin filament sliding velocity across a wide range of ionic strengths (Fig. 2*B*). While increased sliding velocity with dATP have been reported in previous work (1), Fig. 2 demonstrates that dATP significantly increases the interaction between actin and cardiac HMM across a wide range of ionic strength compared with ATP. This further supports the notion that dATP enhances the electrostatic interaction between actin and cardiac myosin relative to ATP.

Table 1. Second-order bimolecular association rate constants for myosin-ADP or myosin-dADP binding with an actin dimer

Reaction distance criteria, nm	Actin-myosin on-rates, $\mu M^{-1} \cdot s^{-1}$		
	Myosin-ADP	Myosin-dADP	Fold change
0.7	0.42	0.82	1.9
0.8	1.66	4.18	2.5
1.0	8.02	22.02	2.7
1.2	21.37	76.84	3.6
2.5	403.10	1431.73	3.6
5.0	3,198.05	4,460.93	1.4

Rate constants were determined by BD simulations, as described in the text and *SI Appendix*. For each nucleotide, as the reaction distance criteria decreases, the on-rate increases nonlinearly. However, the on-rate for dADP-myosin to the actin dimer is consistently greater compared with ADP-myosin for all reaction distance criteria, with the greatest fold change in the range of 1.2–2.5 nm. This strongly supports the notion of an increased electrostatic affinity between actin and myosin induced by dADP.

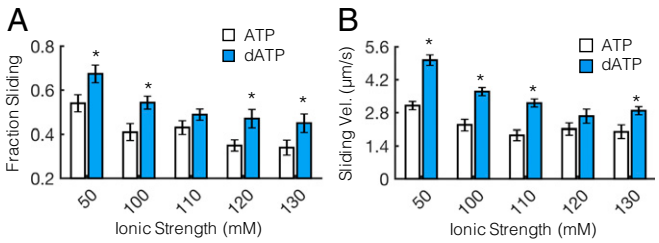

Fig. 2. dATP promotes motility of unregulated F-actin across a range of ionic strengths. (*A*) Fraction of sliding actin filaments is significantly greater across a range of ionic strengths for dATP-bound myosin (blue bars) compared with ATP-bound myosin (white bars). (*B*) (Nonerratic) filament sliding velocity (Vel.) is also significantly increased across a wide range of ionic strengths for dATP compared with ATP, likely owing to a combination of increased ATPase rates and increased actin affinity of dATP-bound myosin compared with ATP. *$P < 0.05$ with an unpaired Student's t test. Error bars represent SEM for $n \geq 12$ slides.

dATP Alters the Resting Structure of Myosin in the Sarcomere. To determine how dATP affects the structure and proximity of myosin to actin within the sarcomere, we used small-angle X-ray diffraction of chemically demembranated (skinned) rat cardiac muscle preparations. Trabeculae or papillary muscles were skinned in relaxing solutions containing either dATP or ATP (*SI Appendix*) and maintained in the same nucleotide species throughout the entire experiment. Measurements were made in physiological (170 mM) and low (100 mM) ionic strength solutions at sarcomere lengths (SLs) of 2.0 μm and 2.3 μm. We note that, as opposed to the IVM experiments, 100 mM is considered low ionic strength in this experimental assay and has been used to alter the actin–myosin interaction sarcomere lattice geometry in previous work (12, 13).

Fig. 3 shows sample two-dimensional X-ray diffraction patterns of resting (pCa 9.0) permeabilized cardiac preparations in ATP or dATP solution (ionic strength = 170 mM). From these images, we quantify (*i*) the intensity and spacing of the myosin-based meridional reflection (I_{M3} and S_{M3}, respectively), which correspond to the periodicity and axial separation distance (respectively) of myosin heads along the thick filament; (*ii*) the filament lattice spacing by measuring the spacing of the 1,0 reflection ($d_{1,0}$) in the equatorial axis; and (*iii*) the ratio of the intensities of the 1,1 and 1,0 equatorial reflections ($I_{1,1}/I_{1,0}$) as an indicator of the radial distribution of myosin mass relative to the thin and thick filaments.

Under physiological ionic strength conditions, in the absence of calcium (pCa 9.0), cardiac muscle with dATP had significantly increased interfilament lattice spacing ($d_{1,0}$) compared with ATP at both short and long SLs (Fig. 4*A*). Interestingly, the $I_{1,1}/I_{1,0}$ intensity ratio was also significantly increased at both SLs (Fig. 4*B*). This suggests that in resting cardiac muscle, dATP causes a shift in the distribution of the mass of the myosin heads away from the thick filament backbone and toward the thin filament.

We then investigated the effects of nucleotide on myosin filament structure by examining the myosin-based meridional X-ray reflections. Cardiac muscle with dATP had a significantly increased S_{M3} compared with ATP-treated muscle at both SLs and $\mu = 170$ mM (Fig. 4*C*), while the I_{M3} did not significantly differ with nucleotide species at either SL (Fig. 4*D*). This suggests that the average axial separation of the myosin heads (i.e., distance along the thick filament backbone) is increased with dATP compared with ATP, but the degree of axial ordering of the myosin heads was not affected.

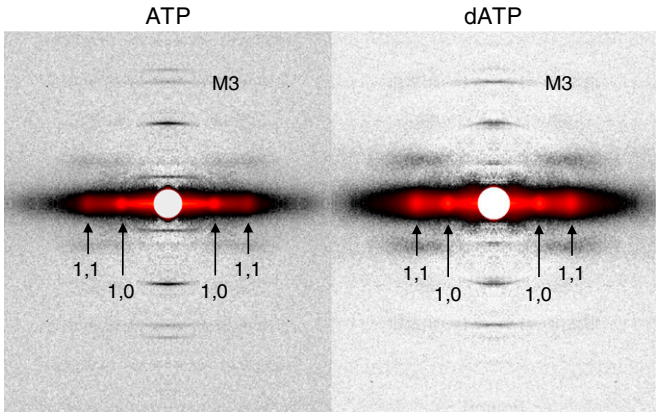

Fig. 3. Sample X-ray diffraction patterns of resting cardiac muscle. Demembranated cardiac trabeculae or papillary muscles from rat right ventricles were exposed to the X-ray beam while bathed in solutions containing ATP (*Left*) or dATP (*Right*) (pCa 9.0, ionic strength = 170 mM, SL = 2.3 μm). In each diffraction pattern, the reflections of interest are labeled. M3, myosin-based meridional reflection due to the axial repeat of myosin crowns; 1,1 and 1,0, equatorial reflections due to the planes of symmetry in the cross-section of the myofilament lattice.

Next, because it has been shown previously that reducing the ionic strength intrinsically increases the affinity of myosin for actin (12), we hypothesized that if the effects of dATP observed at physiological ionic strength on myofilament structure are electrostatic in nature (as suggested by our simulation and IVM data), then lowering the ionic strength would mask these effects such that sarcomere structure would be similar to that with ATP. Indeed, there were no significant differences between cardiac muscle with dATP versus ATP in any of the X-ray reflections investigated at low ionic strength (100 mM) at either SL (Fig. 4 *E–H*). Moreover, these parameters are insensitive to changes in SL at either ionic strength (numerical values of the X-ray reflections in each experimental condition are reported in *SI Appendix*, Table S1).

Thus, our structural data collected in relaxed (pCa 9.0) cardiac muscle preparations demonstrate that, compared with ATP, dATP alters the resting conformation of myosin heads on the thick filament backbone, causing them to be positioned closer to thin filaments with an increased separation distance along the thick filament backbone. Furthermore, the loss of this effect at low ionic strength strongly suggests that the dATP-induced alterations of myofilament structure involve the electrostatic restructuring of myosin predicted by our BD simulations. This conclusion is strengthened by the finding that the effects of dATP on sarcomere and myofilament structure are unaffected by changes in SL in either ionic strength condition.

dATP Induces a Structural Change Similar to Calcium-Mediated Activation of Thick Filaments. Because dATP affects the resting conformation of the of myosin heads in the absence of calcium, it is also possible that myofilament structure and lattice geometry may be affected during activation. As such, we compared the myofilament structure between relaxed (pCa 9.0) and submaximally activated (pCa 5.2) cardiac muscle with dATP versus ATP at SL = 2.3 μm and ionic strength = 170 mM. With ATP, cardiac muscle had a significantly increased lattice spacing during Ca^{2+} activation, while there were no differences in lattice spacing between resting and Ca^{2+}-activated cardiac muscle with dATP (Fig. 5*A*). However, the $I_{1,1}/I_{1,0}$ ratio did increase significantly for both groups during Ca^{2+} activation (Fig. 5*B*), indicating that myosin head position relative to actin filaments was similar during isometric contraction. Interestingly, S_{M3} appeared to be moderately increased for both nucleotides during activation at pCa 5.2, but this change was not statistically significant (Fig. 5*C*). Finally, I_{M3} was significantly reduced upon cardiac muscle activation with ATP, but not dATP (Fig. 5*D*), indicating that the periodicity of thick filaments is less affected during activation with dATP (numerical values are reported in *SI Appendix*, Table S2). Thus, dATP has a greater structural effect on cardiac myofilaments at rest than in (submaximally) Ca^{2+}-activated muscle.

Discussion

A Structural Basis of dATP-Mediated Force Augmentation in Cardiac Muscle: From Single Molecules to the Sarcomere. Our goal in this study was to develop a methodological framework within which we could assess the multiscale mechanisms involved in translating the allosteric effects of small-molecule inotropes on single myosin molecules (8) to altered myofilament ultrastructure and, ultimately, augmented cardiac contractility. Using dATP as a myosin activator, we employed a multifaceted approach that incorporated structural and kinetic information from atomically detailed computational simulations with measurements of myofilament structure and sarcomere lattice geometry using X-ray diffraction techniques. Our results suggest that the augmentation of cardiac contractility by dATP is precipitated by structural responses in myosin that alter its resting conformation in the sarcomere and increase its electrostatic affinity for actin. Taken together, the combination of X-ray diffraction, protein biochemistry,

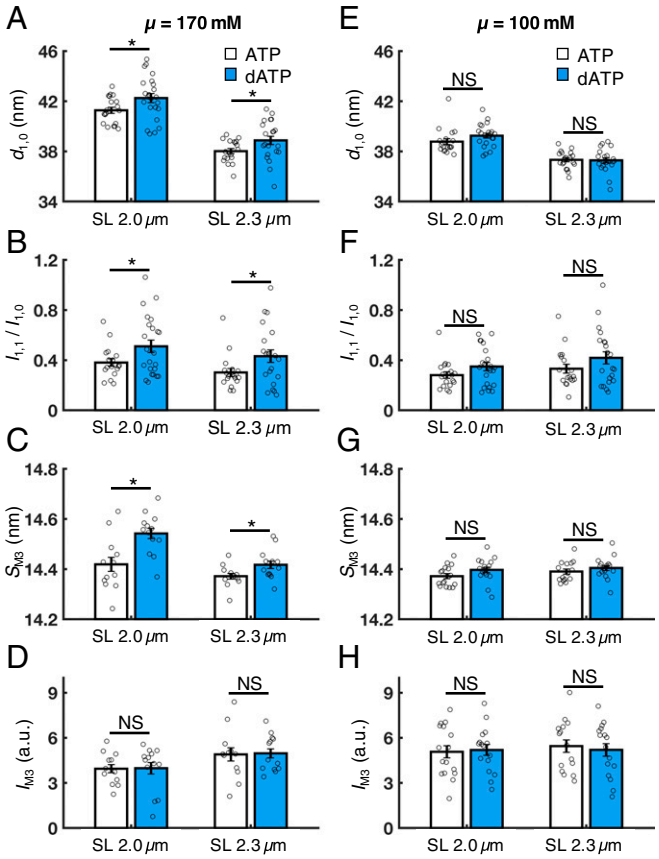

Fig. 4. Effects of dATP on lattice geometry and myofilament structure in resting cardiac muscle (pCa 9.0). At physiological ionic strength (μ = 170 mM), dATP (blue bars) significantly increases the lattice spacing (*A*, $d_{1,0}$), the intensity ratio of the primary equatorial reflections (*B*, $I_{1,1}/I_{1,0}$), and the spacing of the M3 reflection (*C*, S_{M3}) at both short and long SLs compared with ATP (white bars), but does not affect the intensity of the M3 reflection (*D*, I_{M3}) at either SL. However, at low ionic strength (μ = 100 mM), these effects are diminished at both short and long SLs (*E–G*) and the I_{M3} remains unaffected by dATP (*H*). Error bars represent SEM for $n \geq 14$ preparations. *$P < 0.05$. a.u., arbitrary units; NS, not significant. (Numerical values are reported in *SI Appendix*, Table S1.)

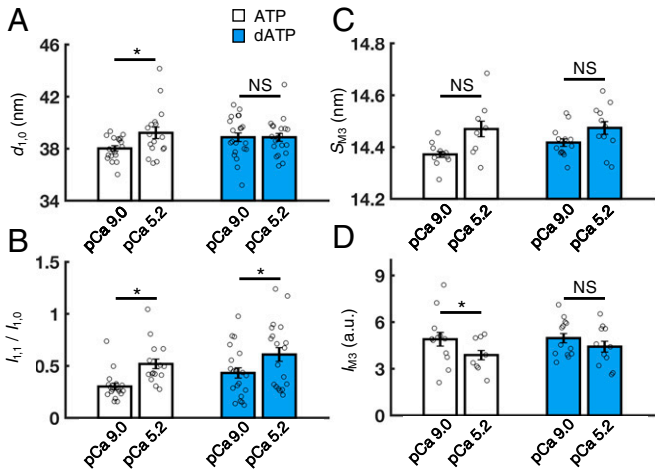

Fig. 5. Effects of dATP on lattice geometry and myosin filament structure in activated muscle (SL = 2.3 μm, μ = 170 mM). Upon activation (pCa 5.2), cardiac muscle with ATP (white bars) has an increased lattice spacing (*A*, $d_{1,0}$), an increased $I_{1,0}/I_{1,1}$ ratio (*B*), no change in the spacing of the M3 reflection (*C*, S_{M3}), and a significantly reduced intensity of the M3 reflection (*D*, I_{M3}) compared with resting muscle (pCa 9.0). However, in preparations containing dATP (blue bars), $I_{1,0}/I_{1,1}$ is significantly increased upon activation, while all other parameters are not significantly different between relaxed (pCa 9.0) and activated (pCa 5.2) states. Error bars represent SEM for $n \geq 8$ preparations. *$P < 0.05$ using a paired Student *t* test. a.u., arbitrary units; NS, not significant. (Numerical values are reported in *SI Appendix*, Table S2.)

and computational approaches used in this study provides a mechanistic bridge between single-myosin allostery, sarcomere structure, and cardiac contractility.

To summarize, our BD simulations of the bimolecular association of an actin monomer with either ADP- or dADP-bound myosin predict that dADP significantly increases the association rate compared with ADP. We attribute this to a dADP-induced conformational change of the actin-binding surface of myosin that exposes more positively charged and polar residues (Fig. 1), effectively increasing its electrostatic affinity for actin. We then verified that dATP induces an electrostatic-based enhancement of the actin–myosin interaction by demonstrating an increased fraction of F-actin sliding and increased sliding velocity in the IVM assay with dATP across a wide range of ionic strengths. Lastly, we used X-ray diffraction analysis to demonstrate that the dATP-induced effects on myosin structure translate into changes in myofilament structure and sarcomere lattice geometry, primarily in resting cardiac muscle. Thus, dATP increases the fraction of myosin motors that are destabilized from the resting conformation compared with ATP, resulting in myosin S1 heads moving closer to actin filaments on average. These changes in resting myosin structure may prime the sarcomere before Ca^{2+}-mediated activation, thereby increasing the probability of strong cross-bridge formation and cycling.

It is important to note that there are limitations to the simplified BD studies performed here. First, the system was assumed to consist of a free-floating myosin S1 head diffusing near a free-floating actin dimer. In the sarcomere, however, the myosin S1 head is tethered to the thick filament and actin is polymerized into F-actin to form the thin filament, restricting the mobility of each protein relative to one another. The simplifications of the model were chosen to optimize computational efficiency, while still elucidating nucleotide-based effects on binding rates. Second, enthalpic force calculations included multipole information up to the dipole level as calculated from electrostatic grids using the Adaptive Poisson–Boltzmann Solver, but the software uses an implicit solvent to maintain computational feasibility, which may affect the overall calculation of electrostatic energies. Therefore, the rates we report here should be considered as qualitative (or pseudoquantitative) evidence for increases in actin–myosin binding due to the presence of dATP rather than exact calculations.

Electrostatic Restructuring of Myosin by dATP Actuates Sarcomeres in Resting Cardiac Muscle. Our combined structural and computational data suggest that dATP induces a conformational change in myosin that results in increased exposure of polar and charged amino acid side chains on its actin-binding surface and this, in turn, promotes actin binding when myosin is in the posthydrolysis, prepowerstroke state. If the mechanism for the altered resting myofilament structure is mainly an increased electrostatic affinity of myosin for actin, then we would expect that compressing the myofilament lattice would enhance these effects by physically bringing actin closer to myosin. This can be done in demembranated muscle either by increasing osmotic compression with dextran or by increasing SL (14, 15). Indeed, for pCa 9.0 and μ = 170 mM, $I_{1,1}/I_{1,0}$ increased by 43% at SL = 2.3 μm (compressed lattice) for dATP compared with ATP, whereas at SL = 2.0 μm (expanded lattice), $I_{1,1}/I_{1,0}$ increased by only 34% (Fig. 4 and *SI Appendix*, Table S1).

However, a number of other mechanisms may also contribute to destabilization of the resting state of myosin motors caused by dATP. First, it is possible that the dATP-induced changes in charge distribution of the actin-binding domain may allosterically affect head–head and/or head–tail interactions (the interacting head motif) of resting myosin motors (16). This could be due to a disruption of either the essential light chain-free motor domain interaction or the blocked motor domain–S2 interaction that has been described in resting skeletal muscle (17). Second, it has recently been shown that multiple phosphorylation pathways that target thick filament proteins also affect the resting structure. For example, phosphorylation of myosin-binding protein C (MyBP-C) repositions myosin heads closer to the actin filaments in demembranated cardiac muscle in the absence of calcium (18, 19), while under normal conditions, MyBP-C interacts with the S2 domain of myosin and/or the thick filament backbone to stabilize the resting state of thick filaments (20, 21). These findings suggest that MyBP-C plays a significant role in modulating the resting myosin filament structure. It is possible that the change in myosin structure with dATP may alter regulation of the MyBP-C–myosin system in the absence of Ca^{2+}. Furthermore, phosphorylation of the regulatory light chain of myosin via myosin light chain kinase (MLCK) also repositions myosin motors closer to actin in resting cardiac muscle (22). This is likely the structural basis of the phosphorylation-dependent increased rate of force development, Ca^{2+} sensitivity of force, and maximum force production in skinned cardiac muscle after treatment with MLCK (22). It is possible that the structural effects of dATP on myosin we present here underpin a similar structural basis of augmented cardiac contractility as these physiological responses.

It has also recently been demonstrated that systolic force development is regulated by a mechanosensing-based mechanism in the thick filament that occurs downstream from calcium-mediated thin filament activation and involves a rapid, feed-forward, and load-dependent recruitment of resting myosin motors for strong cross-bridge binding (23, 24). In the absence of Ca^{2+}, how might the dATP-induced "primed" state of the myosin filament affect such a feed-forward mechanism? The combination of the perturbed resting state of myosin motors and increased electrostatic affinity of actin caused by dATP may work in concert to potentiate cardiac force production both upstream and downstream of Ca^{2+}-mediated thin filament activation by (*i*) increasing the fraction of "actuated" motors (i.e., motors that are positioned closer to actin and primed for strong cross-bridge formation) in the absence of Ca^{2+} and (*ii*) increasing the probability of strong cross-bridge formation and force development upon Ca^{2+}-mediated thin filament activation. Moreover, while the focus of this work is not to examine how a dATP-induced enhancement in cross-bridge formation may influence thin filament activation, there are some interesting potential implications.

For example, given that strongly bound cross-bridges can augment azimuthal displacement of tropomyosin on the thin filament (25–27), it is likely that the enhanced cross-bridge binding via dATP further amplifies thin filament activation. This is supported by the observation that the slope of steady-state force pCa curves (indicative of the cooperativity of activation) is not strongly affected by dATP (figure 3 of ref. 3). To more directly address this question, high-resolution X-ray diffraction images in future experiments may be able to detect changes in the displacement of tropomyosin with either ATP or dATP as the nucleotide.

Clinical Perspectives on Targeting the Cardiac Thick Filament. Advances in X-ray diffraction, protein spectroscopy, and electron microscopy have made it possible to gain high-resolution structural information about cardiac myosin and thick filament structure. Recent studies utilizing these approaches have primarily investigated the structural consequences of myosin-based mutations associated with cardiomyopathy, as well as small-molecule myosin effectors. There are a number of small-molecule–based inotropes targeting cardiac myosin that are currently being developed to treat HF. One inotrope, omecamtiv mecarbil (OM; formally known as CK-1827452 and AMG 423) is currently in phase III clinical trials for treatment of systolic HF. OM selectively binds to myosin and increases the fraction of myosin motors that are strongly bound to actin (28, 29), and may increase the transition from weak to strong actin–myosin interactions without affecting intracellular Ca^{2+} handling (30). Similar to what we report here for dATP, OM perturbs the regulatory state of the cardiac thick filament and causes myosin motors to switch to a more activated state at low levels of Ca^{2+}, where they are more perpendicular to the thick filament backbone (31). Interestingly, despite mobilizing myosin motors in the absence of Ca^{2+}, OM reduces force production at higher Ca^{2+} concentrations in demembranated cardiac muscle (31, 32) and prolongs actomyosin attachment by up to fivefold (33), while dATP increases force at all levels of Ca^{2+} and increases myosin cycling (4). Therefore, dATP has similar beneficial effects on augmenting systolic pressure development as OM; however, in contrast to OM, systole is not prolonged and the rate of pressure decline at the end of systole is enhanced (2, 34).

Methods

All animal experiments were done in compliance with protocols approved by both the University of Washington and the Illinois Institute of Technology Institutional Animal Care and Use Committees and followed the *Guide for the Care and Use of Laboratory Animals* (35). Fourteen adult male Fischer 344 rats were used in the experiments. Details of the material and methods for this work are provided in *SI Appendix*.

ACKNOWLEDGMENTS. This work was supported by NIH Grants R01 HL128368 and R56 AG055594 (to M.R.), NIH Grant U01 HL122199 (to M.R. and A.D.M.), NIH Grant T32-HL007312 (to J.D.P.), a Sackler Scholars Program Fellowship in Integrative Biophysics (to C.-C.Y.), NIH Grant T32-HL105373 (to K.J.M.), NIH Grant K08 HL128826 (to F.M.-H.), and NIH Grant T32-EB1650 (to J.D.M.). This project was supported by Grants 9 P41 GM103622 and 8 P41 GM103426 from the National Institute of General Medical Sciences of the NIH. This research used resources of the Advanced Photon Source, a US Department of Energy (DOE) Office of Science User Facility operated for the DOE Office of Science by the Argonne National Laboratory under Contract DE-AC02-06CH11357.

1. M. Regnier, A. J. Rivera, Y. Chen, P. B. Chase, 2-deoxy-ATP enhances contractility of rat cardiac muscle. *Circ. Res.* **86**, 1211–1217 (2000).
2. S. Kadota *et al*., Ribonucleotide reductase-mediated increase in dATP improves cardiac performance via myosin activation in a large animal model of heart failure. *Eur. J. Heart Fail.* **17**, 772–781 (2015).
3. F. Moussavi-Harami *et al*., 2-Deoxy adenosine triphosphate improves contraction in human end-stage heart failure. *J. Mol. Cell. Cardiol.* **79**, 256–263 (2014).
4. M. Regnier *et al*., Cross-bridge versus thin filament contributions to the level and rate of force development in cardiac muscle. *Biophys. J.* **87**, 1815–1824 (2004).
5. M. Regnier, D. A. Martyn, P. B. Chase, Calcium regulation of tension redevelopment kinetics with 2-deoxy-ATP or low [ATP] in rabbit skeletal muscle. *Biophys. J.* **74**, 2005–2015 (1998).
6. M. Regnier, E. Homsher, The effect of ATP analogs on posthydrolytic and force development steps in skinned skeletal muscle fibers. *Biophys. J.* **74**, 3059–3071 (1998).
7. M. Regnier, D. M. Lee, E. Homsher, ATP analogs and muscle contraction: Mechanics and kinetics of nucleoside triphosphate binding and hydrolysis. *Biophys. J.* **74**, 3044–3058 (1998).
8. S. G. Nowakowski, M. Regnier, V. Daggett, Molecular mechanisms underlying deoxy-ADP.Pi activation of pre-powerstroke myosin. *Protein Sci.* **26**, 749–762 (2017).
9. G. A. Huber, J. A. McCammon, Browndye: A software package for Brownian dynamics. *Comput. Phys. Commun.* **181**, 1896–1905 (2010).
10. E. Homsher, F. Wang, J. R. Sellers, Factors affecting movement of F-actin filaments propelled by skeletal muscle heavy meromyosin. *Am. J. Physiol.* **262**, C714–C723 (1992).
11. M. Furch, M. A. Geeves, D. J. Manstein, Modulation of actin affinity and actomyosin adenosine triphosphatase by charge changes in the myosin motor domain. *Biochemistry* **37**, 6317–6326 (1998).
12. S. Xu, D. Martyn, J. Zaman, L. C. Yu, X-ray diffraction studies of the thick filament in permeabilized myocardium from rabbit. *Biophys. J.* **91**, 3768–3775 (2006).
13. S. Xu, J. Gu, B. Belknap, H. White, L. C. Yu, Structural characterization of the binding of Myosin*ADP*Pi to actin in permeabilized rabbit psoas muscle. *Biophys. J.* **91**, 3370–3382 (2006).
14. D. A. Martyn *et al*., Response of equatorial x-ray reflections and stiffness to altered sarcomere length and myofilament lattice spacing in relaxed skinned cardiac muscle. *Biophys. J.* **86**, 1002–1011 (2004).
15. T. C. Irving, J. Konhilas, D. Perry, R. Fischetti, P. P. de Tombe, Myofilament lattice spacing as a function of sarcomere length in isolated rat myocardium. *Am. J. Physiol. Heart Circ. Physiol.* **279**, H2568–H2573 (2000).
16. L. Alamo *et al*., Three-dimensional reconstruction of tarantula myosin filaments suggests how phosphorylation may regulate myosin activity. *J. Mol. Biol.* **384**, 780–797 (2008).
17. J. L. Woodhead *et al*., Atomic model of a myosin filament in the relaxed state. *Nature* **436**, 1195–1199 (2005).
18. B. A. Colson *et al*., Protein kinase A-mediated phosphorylation of cMyBP-C increases proximity of myosin heads to actin in resting myocardium. *Circ. Res.* **103**, 244–251 (2008).
19. B. A. Colson *et al*., Myosin binding protein-C phosphorylation is the principal mediator of protein kinase A effects on thick filament structure in myocardium. *J. Mol. Cell. Cardiol.* **53**, 609–616 (2012).
20. T. Kampourakis, Z. Yan, M. Gautel, Y.-B. Sun, M. Irving, Myosin binding protein-C activates thin filaments and inhibits thick filaments in heart muscle cells. *Proc. Natl. Acad. Sci. U.S.A.* **111**, 18763–18768 (2014).
21. M. E. Zoghbi, J. L. Woodhead, R. L. Moss, R. Craig, Three-dimensional structure of vertebrate cardiac muscle myosin filaments. *Proc. Natl. Acad. Sci. U.S.A.* **105**, 2386–2390 (2008).
22. B. A. Colson *et al*., Differential roles of regulatory light chain and myosin binding protein-C phosphorylations in the modulation of cardiac force development. *J. Physiol.* **588**, 981–993 (2010).
23. M. Reconditi *et al*., Myosin filament activation in the heart is tuned to the mechanical task. *Proc. Natl. Acad. Sci. U.S.A.* **114**, 3240–3245 (2017).
24. M. Caremani *et al*., Inotropic interventions do not change the resting state of myosin motors during cardiac diastole. *J. Gen. Physiol.* **151**, 53–65 (2019).
25. B. C. W. Tanner, T. L. Daniel, M. Regnier, Filament compliance influences cooperative activation of thin filaments and the dynamics of force production in skeletal muscle. *PLoS Comput. Biol.* **8**, e1002506 (2012).
26. L. Smith, C. Tainter, M. Regnier, D. A. Martyn, Cooperative cross-bridge activation of thin filaments contributes to the Frank-Starling mechanism in cardiac muscle. *Biophys. J.* **96**, 3692–3702 (2009).
27. A. M. Gordon, E. Homsher, M. Regnier, Regulation of contraction in striated muscle. *Physiol. Rev.* **80**, 853–924 (2000).
28. B. H. Greenberg *et al*., Safety and tolerability of omecamtiv mecarbil during exercise in patients with ischemic cardiomyopathy and angina. *JACC Heart Fail.* **3**, 22–29 (2015).
29. F. I. Malik *et al*., Cardiac myosin activation: A potential therapeutic approach for systolic heart failure. *Science* **331**, 1439–1443 (2011).
30. D. A. Winkelmann, E. Forgacs, M. T. Miller, A. M. Stock, Structural basis for drug-induced allosteric changes to human β-cardiac myosin motor activity. *Nat. Commun.* **6**, 7974 (2015).
31. T. Kampourakis, X. Zhang, Y.-B. Sun, M. Irving, Omecamtiv mercabil and blebbistatin modulate cardiac contractility by perturbing the regulatory state of the myosin filament. *J. Physiol.* **596**, 31–46 (2018).
32. L. Nagy *et al*., The novel cardiac myosin activator omecamtiv mecarbil increases the calcium sensitivity of force production in isolated cardiomyocytes and skeletal muscle fibres of the rat. *Br. J. Pharmacol.* **172**, 4506–4518 (2015).
33. M. S. Woody *et al*., Positive cardiac inotrope omecamtiv mecarbil activates muscle despite suppressing the myosin working stroke. *Nat. Commun.* **9**, 3838 (2018).
34. S. C. Kolwicz , Jr *et al*., AAV6-mediated cardiac-specific overexpression of ribonucleotide reductase enhances myocardial contractility. *Mol. Ther.* **24**, 240–250 (2016).
35. National Research Council, *Guide for the Care and Use of Laboratory Animals* (National Academies Press, Washington, DC, ed. 8, 2011).